DOI: 10.1002/chem.200800127

New Layered Rare-Earth Hydroxides with Anion-Exchange Properties

Fengxia Geng,[a, b] Hao Xin,[a] Yoshitaka Matsushita,[c] Renzhi Ma,[a] Masahiko Tanaka,[c] Fujio Izumi,[d] Nobuo Iyi,[a] and Takayoshi Sasaki*[a, b]

Abstract: We report the synthesis of a new series of layered hydroxides based on rare-earth elements with a composition of $RE(OH)_{2.5}Cl_{0.5}\cdot 0.8H_2O$ (RE: Eu, Tb, etc.) through the homogeneous precipitation of $RECl_3\cdot xH_2O$ with hexamethylenetetramine (HMT). Rietveld analysis combined with direct methods revealed an orthorhombic layered structure comprising a positively charged layer of $[RE(OH)_{2.5}(H_2O)_{0.8}]^{0.5+}$ and interlayer Cl^- ions. The Cl^- ions were readily exchangeable for various anions (NO_3^-, SO_4^{2-}, dodecylsulfonate, etc.) at ambient temperature. Photoluminescence studies showed that the compounds display typical RE^{3+} emission. With rare-earth-based host layers and tunable interlayer guests, the new compounds may be of interest for optoelectronic, magnetic, catalytic, and biomedical materials.

Keywords: anions · ion exchange · layered compounds · luminescence · rare-earth elements

Introduction

Layered materials have been the subject of intensive studies in the past few decades because they usually exhibit rich interlayer chemistry, which allows their electronic, magnetic, and optical properties to be modified.[1] For example, novel functional compounds and composites can be obtained from layered materials through a direct ion-exchange method.[2] Although a large variety of layered materials possessing cation-exchange properties (such as cationic clays, metal phosphates and phosphonates, and layered oxides) are known, layered materials that exhibit anion-exchange properties are comparatively rare.[3] Thus far, only hydrotalcite-type layered double hydroxides (LDHs)[4] and some layered hydroxide (or basic) salts[5] have been found to be anion exchangers. The lamellar structure and the anion-exchange properties of LDHs make them attractive for a wide variety of technological applications, for example, as ion exchangers, adsorbents, pharmaceutical stabilizers, and precursors of catalytic materials.[1,6] With a new anion-exchangeable host, striking progress may be anticipated.

Rare-earth compounds, due to the electronic, optical, and chemical characteristics resulting from the 4f shell of their ions, have been widely used in technological applications ranging from high-performance luminescent devices to magnets, catalysts, etc.[7] Their properties are sensitive to the bonding states of the rare-earth ions and strongly depend on the composition and structure. The synthesis of layered rare-earth compounds with interlayer exchangeable guests may be an effective way to control and tune their properties for new technological applications. Among the layered rare-earth hydroxide salts,[8] anion-exchange reactions of lanthanum hydroxide nitrates, $La(OH)_2NO_3$, with some organic anions (acetate, terephthalate, benzoate) were reported.[9] However, the conditions for the exchange of the directly coordinated nitrate anions were somewhat critical, that is, exchange only took place when the reactions were performed

[a] F. Geng,[+] Dr. H. Xin,[+] Dr. R. Ma, Dr. N. Iyi, Prof. T. Sasaki
International Center for Materials Nanoarchitectonics and Nanoscale Materials Center
National Institute for Materials Science
1-1 Namiki, Tsukuba, Ibaraki 305-0044 (Japan)
Fax: (+81) 29-854-9061
E-mail: Sasaki.Takayoshi@nims.go.jp

[b] F. Geng,[+] Prof. T. Sasaki
Graduate School of Pure and Applied Sciences
University of Tsukuba
1-1-1 Tennodai, Tsukuba, Ibaraki, 305-8571 (Japan)

[c] Dr. Y. Matsushita, Dr. M. Tanaka
Beam Line Station
National Institute for Materials Science
1-1-1 Kouto, Sayo-cho, Sayo-gun, Hyogo 679-5148 (Japan)

[d] Dr. F. Izumi
Quantum Beamline Center
National Institute for Materials Science
1-1 Namiki, Tsukuba, Ibaraki 305-0044 (Japan)

[+] These authors contributed equally to the work.

Supporting information for this article is available on the WWW under http://dx.doi.org/10.1002/chem.200800127 or from the author.

at 65 °C for one week. The required severity of the conditions suggested that the reactions might occur through a dissolution–reprecipitation mechanism, rather than a topotactic anion exchange. It is therefore essential to synthesize new layered rare-earth compounds with high anion exchangeability.

Herein, we report the synthesis of new layered hydroxides of rare-earth elements with a composition of $Eu(OH)_{2.5}Cl_{0.5}\cdot 0.8H_2O$ through homogeneous precipitation of $EuCl_3\cdot x H_2O$ with hexamethylenetetramine (HMT) upon heating to reflux. The layered hydroxides are typically well crystallized as highly developed rectangular platelets of 1–2 μm in size. Rietveld analysis combined with direct methods revealed an orthorhombic layered structure comprising positively charged layers of $[Eu_8(OH)_{20}(H_2O)_{6.4}]^{0.5+}$ and interlayer Cl^- ions. The interlayer Cl^- ions are readily exchangeable for various inorganic (NO_3^-, SO_4^{2-}) and organic ($C_{12}H_{25}OSO_3^-$) ions at ambient temperature. This new compound opens up the possibility to explore the unique properties of rare-earth compounds through a direct ion-exchange process.

Results and Discussion

Synthesis and characterization of $Eu(OH)_{2.5}Cl_{0.5}\cdot 0.8H_2O$: Figure 1a shows a typical TEM image of the synthesized Eu compound. The sample adopted a rectangular platelike morphology with a thickness of about 20 nm. The platelets were uniform in lateral size, with a length of about 2 μm and a width of about 1 μm. The selected-area electron diffraction (SAED) pattern taken from an individual platelet lying on a copper grid is shown in Figure 1b. The different brightnesses of some spots in the SAED pattern indicate the possible presence of a superlattice structure. Specifically, the brighter spots correspond to a fundamental cell in a pseudohexagonal symmetry ($a_f = 3.7$ Å), while the weaker ones correspond to a rectangular supercell ($a_s = 2\sqrt{3}a_f = 13.1$ Å; $b_s = 2a_f = 7.4$ Å). The relationship between the fundamental cell and the supercell is schematically interpreted in Figure 1c. The fundamental hexagonal cell might indicate a hexagonal arrangement of rare-earth atoms closely related to a brucite-like ($Mg(OH)_2$) or LDH-like ($[M^{2+}_{1-x}M^{3+}_x(OH)_2]^{x+}$; M: metal) host layer (Eu···Eu: 3.7 Å). A possible occupancy fluctuation or position deviation from the ideal brucite structure might give rise to a rectangular supercell, containing eight Eu atoms, as deduced from the cell dimensions.

All of the reflections of the synchrotron XRD pattern can be indexed in a single orthorhombic unit cell with lattice parameters of $a = 12.92(1)$, $b = 7.38(1)$, and $c = 8.71(1)$ Å (see Figure S1 in the Supporting Information). It is noteworthy that the ratio of a to b is not exactly equal to $\sqrt{3}$, which implies that the fundamental cell is not of perfect hexagonal symmetry as in the ideal brucite structure. The a and b values are consistent with those determined by SAED measurements, which indicates that the platelets were lying on their {001} crystal planes and the SAED pattern was taken along the [001] zone axis. The well-developed platelet morphology should be derived from the preferred in-plane crystallographic growth habit of the orthorhombic symmetry. The sharp reflections in the XRD pattern suggest the highly crystalline nature for the product. The prominent intensity of basal reflections 001 and 002 in the X-ray pattern is notable and indicates a preferred orientation caused by the thin platelet morphology.

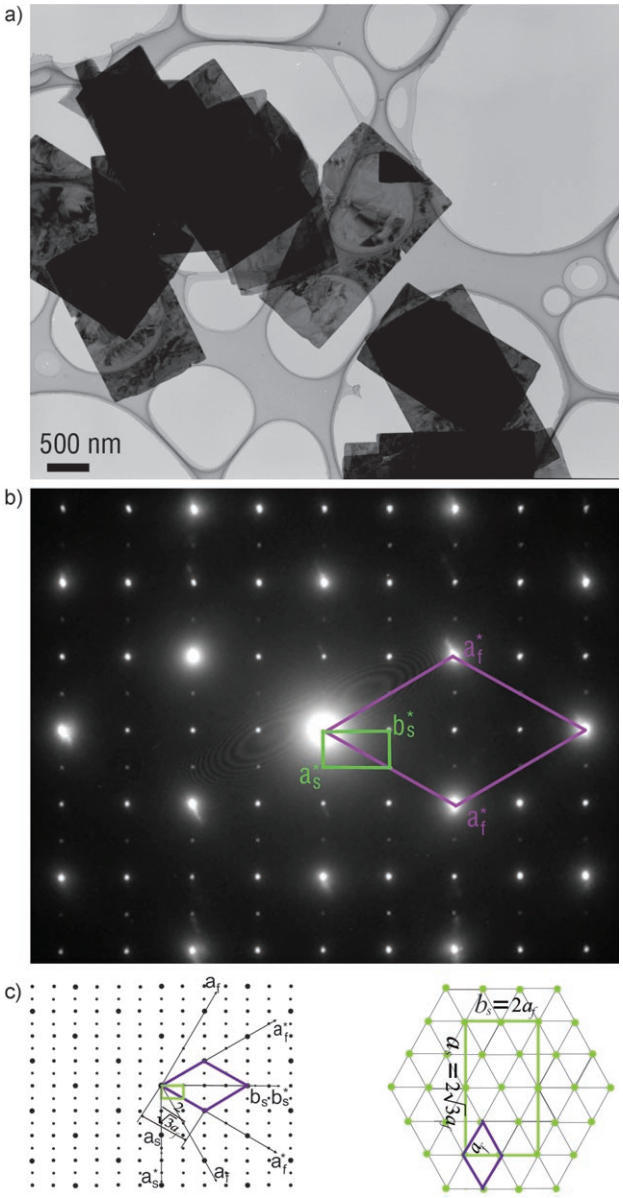

Figure 1. a) Representative TEM image of the platelets, b) SAED pattern of a platelet, and c) relationship between the fundamental cell and the superlattice cell. a_f: axis of fundamental hexagonal cell in the real space; a_s, b_s: a and b axes of the superlattice cell in the real space, respectively. Labels with asterisks are the corresponding reciprocal axes.

Crystal structure of $Eu(OH)_{2.5}Cl_{0.5}\cdot 0.8H_2O$: Examination of the XRD indices suggests a systematic absence of $h = 2n+1$ for $h00$ and $k = 2n+1$ for $0k0$, which indicates $P2_12_12$ to be

a possible space group.[10] However, due to severe overlaps of peak positions, other space-group choices such as $P222$ and $Pmm2$ cannot be completely excluded. All of these three possible space groups were tested in a Le Bail intensity extraction, which does not require a structural model, and the space group of $P2_12_12$ was found to yield the best fitting results. The structure was then solved in the space group of $P2_12_12$. On the basis of the chemical analysis results, the elemental composition was estimated to be $Eu(OH)_{2.41}Cl_{0.49}(CO_3)_{0.05}\cdot 0.78H_2O$ (elemental analysis: calcd (%): Eu 66.83, OH^- 18.02, Cl^- 7.64, C 0.26, H_2O 6.18%; found (%): Eu 65.5, OH^- 17.7, Cl^- 7.5, C 0.25, H_2O 6.1%). As it was determined from the electron-diffraction study that there are eight Eu atoms in one unit cell, the formula unit was determined as $Z=8$, that is, $Eu_8(OH)_{19.28}Cl_{3.92}(CO_3)_{0.40}\cdot 6.24H_2O$. To simplify the structure determination, the carbonate charge was transformed into a hydroxy charge and then the formula unit was taken as $Eu_8(OH)_{20}Cl_4\cdot 6.4H_2O$. A direct method by using the program EXPO2004[11] was first applied to derive the positions of the eight Eu atoms. The other lighter species (OH, H_2O, Cl) were estimated through an electron-density distribution analysis by employing the maximum-entropy method (MEM)/Rietveld technique.[12] A layered structure model was generated, as shown in Figure 2a. The RIETAN-FP[13] software was subsequently used to refine the structure parameters. Refined fractional coordinates are listed in Table 1. The three-dimensional electron-density distribution is visualized in Figure 2b, which corresponds well with the atomic structure model. One notable feature is that the electron density corresponding to the interlayer Cl^- ions has a slightly distorted spherical distribution, which suggests that the Cl^- ions might also be well ordered in the gallery; this is different from other layered materials, which usually exhibit disordered interlayer anions.[14] The full profile of the experimental, calculated, and difference patterns is shown in Figure 2c. The final R factors were obtained as $R_{wp}=2.00$ ($S=0.5072$), $R_p=1.49$, $R_I=4.00$, and $R_F=1.59\%$. The satisfactory low R factors provide strong evidence for the validity of the structure model.

Table 1. Refined structure parameters for $Eu(OH)_{2.5}Cl_{0.5}\cdot 0.8H_2O$ showing fractional coordinates (x, y, z) and occupancies (g).[a]

Atom	Site	g	x	y	z
Eu1	4c	1	0.2739(1)	0.2503(13)	0.9343(2)
Eu2	2b	1	0	0.5	0.9326(4)
Eu3	2a	1	0	0	0.9194[b]
OH1	4c	1	0.470(1)	0.266(5)	0.921(2)
OH2	4c	1	0.097(1)	0.256(12)	0.825(2)
OH3	4c	1	0.162(6)	0.441(7)	0.079(8)
OH4	4c	1	0.667(6)	0.444(7)	0.925(8)
OH5	4c	1	0.132(1)	0.733(6)	0.865(2)
H_2O1	4c	1	0.206(1)	0.793(2)	0.337(2)
H_2O2	2b	0.7220	0	0.5	0.647(9)
H_2O3	2a	0.4780	0	0	0.625(14)
Cl	4c	1	0.1380(5)	0.2147(12)	0.4179(9)

[a] Space group: $P2_12_12$ (no. 18); Unit cell parameters: $a=12.9152(3)$, $b=7.3761(1)$, $c=8.7016(3)$ Å. Numbers in parentheses are standard deviations. All of temperature factors (B_{iso}) were fixed at 1.0 $Å^2$ for Eu and 2.0 $Å^2$ for other sites during refinement. At the final refinement stage, the occupancies of the water molecules were also fixed according to the composition determined by chemical analysis. [b] The coordinates of Eu3 are fixed at the value obtained by direct methods because the space group $P2_12_12$ (no. 18) is non-centrosymmetric.

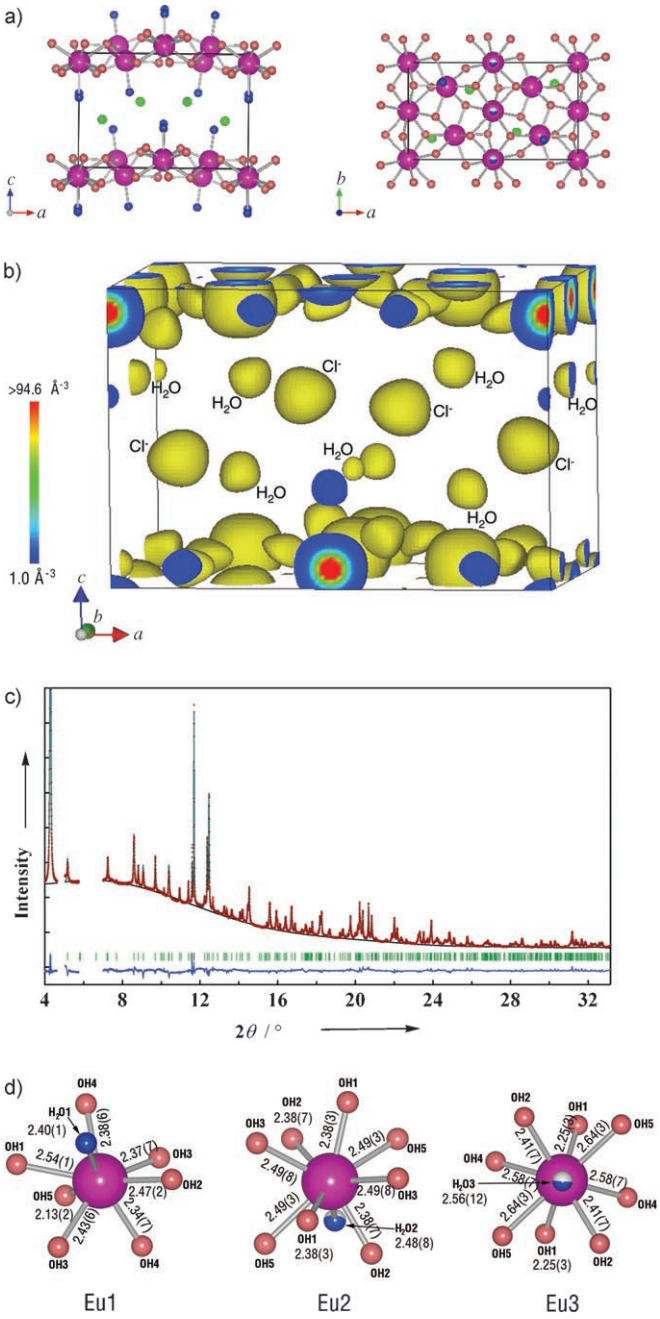

Figure 2. a) Crystal structure for $Eu(OH)_{2.5}Cl_{0.5}\cdot 0.8H_2O$ projected along the [010] and [001] directions. Eu, OH, H_2O, and Cl species are represented by pink, orange, blue, and green balls, respectively. b) Three-dimensional electron-density distribution, where the isosurface level is 1.0 $Å^{-3}$. On the incisions (the spectrum form): red indicates the maximum and blue indicates the minimum. c) Full-profile Rietveld refinement pattern. The red, green, and blue lines represent the experimental, calculated, and difference profiles, respectively. d) Local environments of the three types of Eu site in the host layer.

The refinement results revealed some important structural features of the new layered rare-earth hydroxide. The structure consists of $[Eu_8(OH)_{20}(H_2O)_{6.4}]^{4+}$ cationic layers with chloride ions residing in the gallery to compensate for the positive charge. There are two kinds of site assignment for the Eu cations: the first occupies 4c (0.2739, 0.2503, 0.9343) sites with eight-coordination to seven hydroxy groups and one water molecule; the other resides on 2a (0, 0, 0.9194) or 2b (0, 0.5, 0.9326) sites with nine-coordination to eight hydroxy groups and one water molecule. The three different coordination environments are shown in Figure 2d. In all of the coordinations, every hydroxy group is bonded to three Eu atoms within a reasonable distance range of 2.1–2.6 Å. The $H_2O\cdots$Eu distances in the 8- and 9-coordination environments are 2.39(2) and 2.56(12)/2.48(8) Å, respectively. The site assignments produce alternating rows of Eu atoms, which form layers parallel to the *ab* plane. The position deviation of the Eu atoms from the ideal in-plane hexagonal arrangement agrees well with the SAED study. That is, although a fundamental cell of hexagonal symmetry might be approximately acknowledged, it corrugates in the *z* [001] direction, which results in an orthorhombic supercell. The rare-earth host layer is similar to that previously observed in the metal–organic framework of $[RE_4(OH)_{10}(H_2O)_4]_nA_n$ (RE: rare-earth ions; A: intercalated organic anions 2,6-naphthalenedisulfonate (NDS^{2-}) and 2,6-anthraquinonedisulfonate ($AQDS^{2-}$)),[15] although the layers in the earlier structure were pillared by rigid organic anions of NDS^{2-} or $AQDS^{2-}$ and were kinetically favored only by small rare-earth ions (Dy, Ho, Yb, Lu, and Y). For the current series containing simple inorganic anions, besides $Eu(OH)_{2.5}Cl_{0.5}\cdot 0.8H_2O$, the synthesis can be extended to obtain pure layered compounds of Sm, Gd, Tb, Dy, Ho, Er, and Y. It also produces mixture of $Nd(OH)_{2.5}Cl_{0.5}\cdot xH_2O$ and $Nd(OH)_3$ for Nd.

Unlike the di- and trivalent cation combination in the planar LDH host layers of $[M^{2+}_{1-x}M^{3+}_x(OH)_2]^{x+}$, there is only a single trivalent rare-earth cationic species in the current corrugated host layer. Furthermore, in the typical LDH structure, all of the anions and water molecules are usually located in the middle plane of the interlayer gallery. A hydrogen-bonding network develops between the interlayer species and both neighboring octahedral layers. There are a few exceptions in which the interlayer species might be distributed between two sublayers (deviated from the middle plane) in such a way that none of them is able to have direct hydrogen-bonding contact with both neighboring octahedral sheets at the same time.[16] In the present structure, the chloride anions at the 4c position (0.1380, 0.2147, 0.4179) also form two sublayers with Cl to Eu interatomic distances of 4.567 (8) Å for the nearer host sheet and of 4.832 (8) Å for the other. This implies that the Cl^- ions might only have a strong interaction with the nearer host sheet. Another noticeable difference from LDH is that the water molecules are directly coordinated to the Eu atoms forming the polyhedra instead of being intercalated freely in the gallery. Rare-earth elements generally have a strong affinity to oxygen atoms. Since the synthesis was done in aqueous solution, direct coordination of water to the rare-earth cations is assumed to be reasonable. Possibly due to this direct-coordination relationship, the water molecule appears to be vital in stabilizing the layer structure. This is consistent with the experimental observation that variation in the humidity may bring dramatic phase changes to the structure. For example, if the sample is dried too much, the layered phase may collapse.

Photoluminescence properties of $Eu(OH)_{2.5}Cl_{0.5}\cdot 0.8H_2O$: The room-temperature excitation and emission spectra for $Eu(OH)_{2.5}Cl_{0.5}\cdot 0.8H_2O$ are shown in Figure 3; the excitation

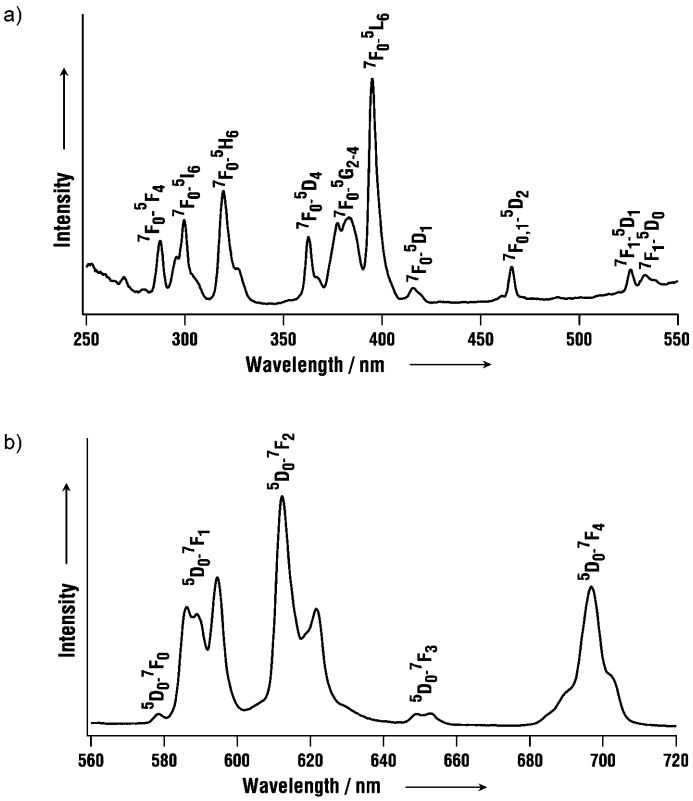

Figure 3. Photoluminescence a) excitation and b) emission spectra of $Eu(OH)_{2.5}Cl_{0.5}\cdot 0.8H_2O$ at room temperature, monitored at 612 nm and 395 nm, respectively.

spectrum was obtained by monitoring within the $^5D_0$–$^7F_2$ lines (612 nm) and the emission spectrum was measured through intra-$4f^6$ (395 nm) direct excitation. The excitation spectrum consists of a series of sharp lines ascribed to intra-$4f^6$ transitions within the Eu^{3+} $4f^6$ electronic configuration. The emission spectrum displays typical $^5D_0$–^7F_J ($J=0$–4) transitions at 578.4, 594.6, 612.4, 649.0, and 696.8 nm, respectively. Luminescence from higher excited levels such as $^5D_1$ was not detected, a result that indicates a very efficient nonradiative relaxation to the $^5D_0$ level. The intensities of different $^5D_0$–^7F_J transitions and the splitting of these emission peaks are usually used to probe the environment of the

Eu^{3+} ion because they strongly depend on the local symmetry of the crystal field. There are two main features in the emission spectrum. First, the hypersensitive $^5D_0$–$^7F_2$ transition peak at 612 nm appears to be dominant. Theoretically, if the Eu^{3+} ion occupies an inversion symmetry site in the crystal lattice, the magnetic dipole transition $^5D_0$–$^7F_1$ (around 590 nm) is the dominant transition; otherwise, the electric dipole transition $^5D_0$–$^7F_2$ (around 610–620 nm) becomes dominant. The observed features in the emission spectrum suggest that there is no inversion center in the present structure. Second, the $^5D_0$–$^7F_1$ and $^5D_0$–$^7F_2$ emissions split into three and two peaks, respectively; these results indicate a lower symmetry of crystal field around the Eu^{3+} ions. The structure determination has shown that there are two local sites available for the Eu^{3+} coordination, namely, the 4c position with eight-coordination and the 2a/2b position with nine-coordination, in local symmetry groups of C_1 and C_{4v}, respectively. Both of the two sites have a low symmetry with no inversion center, which is compatible with the split transition peaks in the photoluminescence emission spectrum.

Anion exchange of $Eu(OH)_{2.5}Cl_{0.5}\cdot 0.8H_2O$: The interlayer Cl^- ions were readily exchanged with other inorganic and organic anions at room temperature. Figure 4 shows the

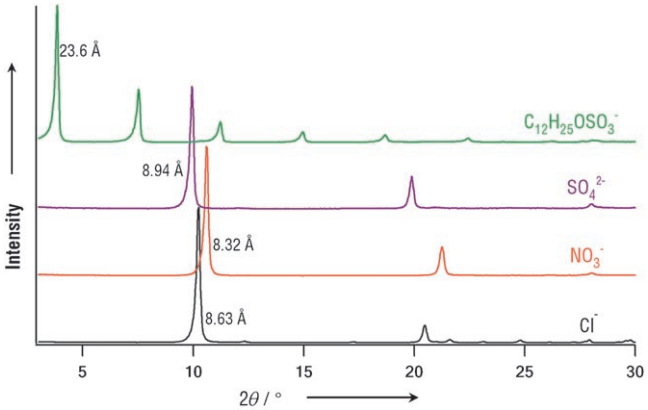

Figure 4. XRD patterns of the as-obtained Cl^- product and those formed after anion exchange with NO_3^-, SO_4^{2-}, and $C_{12}H_{25}OSO_3^-$.

XRD pattern of the as-synthesized product in comparison with those of samples after exchange with NO_3^-, SO_4^{2-}, and $C_{12}H_{25}OSO_3^-$. The basal spacing, 8.63 Å for the pristine Cl^- form, shifted to 8.32 Å nm for NO_3^- and 8.94 Å for SO_4^{2-}. For the large-organic-anion exchange (DS^-), basal series peaks corresponding to a distance of 23.6 Å can be clearly discerned. The diffraction peaks were sharp, which indicates that the high crystallinity was maintained during the exchange procedures. SEM observations showed that the rectangular morphology was well retained (see Figure S2 in the Supporting Information). FTIR measurements also confirm the nearly complete exchange of the anionic species (Figure 5). The spectra for the 3 exchanged products have

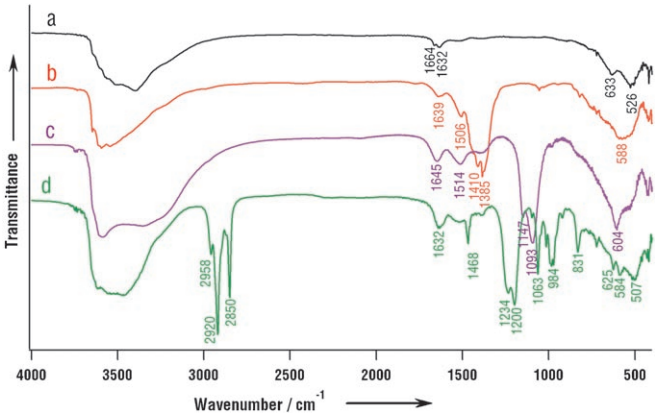

Figure 5. FTIR spectra for a) the as-prepared Cl^- form and the b) NO_3^-, c) SO_4^{2-}, and d) $C_{12}H_{25}OSO_3^-$ samples obtained by the anion-exchange process.

similar vibration bands at approximately 3500, 1650, and 620 cm^{-1}. The band at around 3500 cm^{-1} is attributable to the stretching vibration of the O–H bond, ν(OH), which indicates the presence of hydroxy ions because of the metal–OH layer in the crystal. The peak at around 1650 cm^{-1} is due to the bending mode of the water molecules. The absorptions in the low-frequency region, below 620 cm^{-1}, may be ascribed to Eu–O stretching/bending vibrations. Absorption bands that can be assigned to the interlayer anion are also observed. The sharp and strong absorption peaks in spectrum b at 1385 cm^{-1} and 1410 cm^{-1} are assignable to the D_{3h}, ν3 vibration mode of the NO_3^- ions and the C_{2v}, ν4 asymmetric stretch of O–NO_2, respectively. The bands in spectrum c at 1093 and 1147 cm^{-1} are derived from the SO_4^{2-} ions. The strong bands in spectrum d at 2920 and 2850 cm^{-1} are due to the asymmetric and symmetric CH_2 stretching vibrations, respectively, in the alkyl chain of dodecylsulfate, whereas the relatively weak band at 2958 cm^{-1} is due to the stretching vibration of the terminal CH_3 group of the hydrocarbon tail; the band occurring near 1470 cm^{-1} in the spectra arises from the CH_2 bending (or scissor) mode; the series of absorbance bands in the range of 1300–900 cm^{-1} are due to the stretching mode of the sulfate (OSO_3^-) ions. These assignments clearly indicate the incorporation of these anions. The higher anion exchangeability of the new layered rare-earth hydroxide can be well understood when we compare the structure with that of previous hydroxy salts such as $La(OH)_2NO_3$.[8] For $La(OH)_2NO_3$, one oxygen atom of the interlayer nitrate anion (NO_3^-) is directly coordinated to the lanthanum atoms, whereas in the current structure, the interlayer Cl^- ion acts as a counterion and is prone to exchange by other anions.[17]

Conclusion

In conclusion, we have successfully synthesized a series of new layered rare-earth hydroxides, which are composed of a positively charged layer of $[RE_8(OH)_{20}(H_2O)_{6.4}]^{4+}$ and inter-

layer Cl^- ions. Photoluminescence studies showed that the present materials display typical RE^{3+} emission, which may be of interest for optoelectronic devices. A unique property of the new layered rare-earth hydroxides is that the interlayer Cl^- ions were readily exchangeable for various anions (NO_3^-, SO_4^-, $C_{12}H_{25}OSO_3^-$, etc.); this offers advantages for modifications with other anions. The anion-exchangeable layered rare-earth hydroxides enrich the family of layered hosts in one aspect and may hold great potential applications by uniting the advantages of both anion exchangers and optically interesting hosts on the other.

Experimental Section

Synthesis: The preparation was performed in a two-neck flask equipped with a reflux condenser under a nitrogen flow. Rare-earth chloride ($RECl_3{\cdot}xH_2O$), NaCl, and HMT were dissolved in Milli-Q water (1000 mL) at final concentrations of 5, 65, and 80 mM, respectively. The mixed solution was heated to reflux with continuous magnetic stirring and a nitrogen atmosphere. White streaming lines were observed in the solution after one hour of reaction; these lines indicate the formation of crystallites in an anisotropic shape. The product was filtered, washed with water and ethanol several times, and finally dried at room temperature with a controlled humidity of 70%. Special attention needed to be paid during the sample collection. If water was removed excessively (for example, by collecting the sample at a very low humidity), the product was found to change into an amorphous or very low crystalline phase.

Sample characterization: The morphology and dimensions of the samples were examined by using a JEOL JSM-6700F field-emission scanning electron microscope. Transmission electron microscopy characterizations and selected-area electron diffraction were performed on a JEOL JEM-1010 transmission electron microscope at an acceleration voltage of 100 kV. High-resolution synchrotron powder X-ray diffraction data for structure determination were recorded on the BL15 instrument of the Spring8 synchrotron radiation facility ($\lambda = 0.65297$ Å). XRD data of samples, for example, anion-exchanged phases, were recorded on a Rigaku Rint-2000 diffractometer equipped with a graphite-monochromatized $Cu_{K\alpha}$ radiation source ($\lambda = 1.5405$ Å). The Eu content in the sample was determined by inductively coupled plasma (ICP) atomic emission spectrophotometry (Seiko SPS1700HVR instrument) after a weighed amount of sample was dissolved in an aqueous HCl solution. The OH content was obtained by neutralization back-titration after the sample had been dissolved in 0.1 N standard H_2SO_4. The Cl content was quantified by the ion-electrode method, with DKK IM-40S as the concentration meter, DKK CL-125B as the ion electrode, and DKK RE-2 as the reference electrode. The carbon content was measured on a LECO RC-412 analyzer. The water content was deduced by thermogravimetry. Fourier transform infrared spectra over a range of 400–4000 cm^{-1} were measured on a Varian 7000e FTIR spectrophotometer equipped with a liquid-nitrogen-cooled MCT detector by using the KBr pellet technique. Room-temperature excitation and emission spectra were obtained on a Hitachi F-4500 fluorescence spectrophotometer.

Structure determination: First, the integrated intensities were extracted by using the Le Bail method with the Rietveld program RIETAN-2000. In this procedure, no reference to a structure model is needed. The extracted integrated intensities were then refined and repartitioned by the maximum-entropy Patterson program ALBA to reach more reliable values. The structure factors obtained were introduced into the direct-method program EXPO2004. The positions of the rare-earth atoms could be readily derived. Those of other atoms were estimated by an electron-density distribution analysis by the MEM/Rietveld procedures. The structure was refined by using the RIETAN-FP program. The electron-density distribution was determined by MEM methods by using the values of F_0 estimated after refinement with the PRIMA program. The density map was examined carefully and modifications of the structure model were incorporated if additional peaks were found in the density map. The refinement was terminated when the R factors no longer decreased appreciably and the structure model agreed well with the density maps.

Anion-exchange reactions: A sample in the Cl^- form (0.2 g) was dispersed into an aqueous solution (200 cm^3) of 1 M $NaNO_3$, 1 M Na_2SO_4, or 0.5 M sodium dodecylsulfate (SDS, $C_{12}H_{25}OSO_3Na$). The reaction vessel was tightly capped and shaken for two days at ambient temperature.

Acknowledgements

This work was supported by a CREST grant of the Japan Science and Technology Agency (JST).

[1] B. Sels, D. De Vos, M. Buntinx, F. Pierard, A. Kirsch-De Mesmaeker, P. Jacobs, *Nature* **1999**, *400*, 855–857.
[2] J. H. Lee, S. W. Rhee, D. Y. Jung, *Chem. Mater.* **2006**, *18*, 4740–4746.
[3] H. Nishizawa, K. Yuasa, *J. Solid State Chem.* **1998**, *141*, 229–234.
[4] S. Miyata, *Clays Clay Miner.* **1983**, *31*, 305–311.
[5] M. Meyn, K. Beneke, G. Lagaly, *Inorg. Chem.* **1993**, *32*, 1209–1215.
[6] P. S. Braterman, Z. P. Xu, F. Yarberry in *Handbook of Layered Materials* (Eds.: S. M. Auerbach, K. A. Carrado, P. K. Dutta), Marcel Dekker, **2004**, pp. 373–474.
[7] G.-Y. Adachi, N. Imanaka, *Chem. Rev.* **1998**, *98*, 1479–1514.
[8] J. M. Haschke, *Inorg. Chem.* **1974**, *13*, 1812–1818.
[9] S. P. Newman, W. Jones, *J. Solid State Chem.* **1999**, *148*, 26–40.
[10] The forbidden diffraction spots of $h00$ ($h = 2n+1$) and $0k0$ ($k = 2n+1$) in $P2_12_12$ were observed in the SAED pattern. This discrepancy may be derived from the very small thickness of the sample and a possible stacking disorder; that is, reciprocal lattices become elongated/rod-shaped along the c^* direction and give rise to these relatively weak forbidden spots.
[11] A. Altomare, R. Caliandro, M. Camalli, C. Cuocci, C. Giacovazzo, A. G. G. Moliterni, R. Rizzi, *J. Appl. Crystallogr.* **2004**, *37*, 1025–1028.
[12] F. Izumi, *J. Ceram. Soc. Jpn.* **2003**, *111*, 617–623.
[13] F. Izumi, T. Ikeda, *Mater. Sci. Forum* **2000**, *198*, 321–324.
[14] A. V. Besserguenev, A. M. Fogg, R. J. Francis, S. J. Price, D. O'Hare, V. P. Isupov, B. P. Tolochko, *Chem. Mater.* **1997**, *9*, 241–247.
[15] F. Gándara, J. Perles, N. Snejko, M. Iglesias, B. Gómez-Lor, E. Gutiérrez-Puebla, M. A. Monge, *Angew. Chem.* **2006**, *118*, 8166–8169; *Angew. Chem. Int. Ed.* **2006**, *45*, 7998–8001.
[16] J. W. Wang, A. G. Kalinichev, J. E. Amonette, R. J. Kirkpatrick, *Am. Mineral.* **2003**, *88*, 398–409.
[17] In the last stage of drafting this paper, we found a recent article [L. J. McIntyre, L. K. Jackson, A. M. Fogg, *Chem. Mater.* **2008**, *20*, 335–340] on a similar compound with the stoichiometry of $Ln_2(OH)_5(NO_3){\cdot}xH_2O$ (Ln: Gd–Lu, Y; $x \approx 1.5$). Gd marks the limit for the compounds in that paper. The similar compositions suggest some relationship to the materials in this paper, although their structure was not described.

Received: January 22, 2008
Published online: August 27, 2008

